This article has been accepted for publication in a future issue of this journal, but has not been fully edited. Content may change prior to final publication. Citation information: DOI 10.1109/TIM.2019.2941036, IEEE Transactions on Instrumentation and Measurement

Comparison of Multiple Methods for Obtaining PΩ Resistances with Low Uncertainties

Kwang Min Yu, Dean G. Jarrett*, *Senior Member, IEEE,* Albert F. Rigosi, Shamith U. Payagala, and Marlin E. Kraft

***Abstract*—Capabilities for high resistance determinations are essential for calibration of currents below 1 pA, as typically requested in several applications, including semiconductor device characterization, single electron transport, and ion beam technologies. This need to calibrate low currents warrants the expansion of accessible values of high resistance. We present several methods for measuring resistances on the PΩ scale, namely potentiometry, dual source bridge measurements, and teraohmmeter usage, all of which are subsequently compared to theoretical calculations. These methods were used to measure four 1 PΩ resistances, one 10 PΩ resistance, and one 100 PΩ resistance, all generated by wye-delta networks containing three resistance elements. The differences between the experimentally obtained values and the theoretical values typically agree within 1 % for 1 PΩ, 10 PΩ and 100 PΩ resistances and the measurement uncertainties for the three techniques were estimated to be between 0.4 % to 4.8 % for 1 PΩ, 2.8 % to 5.6 % for 10 PΩ, and 4.4 % to 10.2 % for 100 PΩ.**

***Index Terms*— standard resistor, high resistance, wye-delta transform, dual source bridge**

I. Introduction

THERE are a number of high resistance applications that require correspondingly high resistance measurements, typically on the order of 1 TΩ or higher, such as testing printed circuit board insulation, determining the resistivity of insulating materials or semiconductors, and assessing voltage coefficients of high-valued resistors. Some of these requirements even call for the determination of 1 PΩ to 100 PΩ, prompting many national metrology institutes (NMIs) to participate in international key comparisons for high resistances such as CCEM.EM-K2 [1], SIM.EM-K2 [2], EURAMET.EM-K2 [3], EURAMET.EM-S32 [4], and APMP.EM-K2 [5]. Capabilities for high resistance determinations are also essential for calibration of low currents below 1 pA, usually needed for a myriad of applications, including, but not limited to: semiconductor device characterization, single electron transport, and ion beam technologies. Furthermore, specialized commercial high resistance meters, such as teraohmmeters (TM) [6] and electrometers have resistance measurement ranges up to 10 PΩ. Therefore, a need is present to calibrate those ranges using high resistance standards up to 10 PΩ. There are inherent limits to methods involving dual source bridges (DSBs) [7-10], DC calibrators and digital multimeters (DMMs) [11-12], which are used to measure up to 100 TΩ. And although there has been recently reported work on making 1 PΩ measurements using a DSB [13-14], there is still no method to calibrate higher resistances than 10 PΩ.

Because commercial resistance standards and specially-made Hamon transfer standards [15] also have resistances limited to a maximum value of 100 TΩ, T-networks may be constructed using wye-delta (Y-Δ) transformations [16-18], to make resistances larger than 100 TΩ. In addition to using Y-Δ transformations, which serve as the basis of our calculations, we also employ a potentiometric method with minimal leakage to measure 1 PΩ to 100 PΩ resistances simply and accurately. This first experimental method is later compared with measurements from a DSB and a TM for 1 PΩ to 100 PΩ resistances, bearing in mind that the latter resistances are *effective* values only.

II. Wye-delta networks for high resistances and their uncertainties

A. Construction of PΩ, 10 PΩ and 100 PΩ Resistances

Generally, it is difficult to produce 1 PΩ, 10 PΩ and 100 PΩ resistances using commercial component resistors because the highest commercial resistance standard available is at the 100 TΩ level. Thus, resistances higher than 1 PΩ can be made using Y-Δ transformations. Illustrations of the pre- and post-transformed networks are shown in Figure 1 (a) and (b), respectively. The high resistances R, R_a, and R_b are given by:

$$R = \frac{R_1 \times R_2}{R_0} + R_1 + R_2$$
$$R_a = \frac{R_1 \times R_0}{R_2} + R_1 + R_0$$
$$R_b = \frac{R_2 \times R_0}{R_1} + R_2 + R_0 \quad (1)$$

Manuscript received June 7, 2019; revised XX. For a subset of the author list, this work was prepared as part of their official duties for the U. S. Government. *Asterisk indicates corresponding author.*

K. M. Yu is with the Korea Research Institute of Standards and Science, Yusong, Daejon, 305-600, Korea (email: kmyu@kriss.re.kr).

D. G. Jarrett, S. U. Payagala, A. F. Rigosi, and M. E. Kraft are with the National Institute of Standards and Technology, Gaithersburg, MD 20899, USA (e-mails: dean.jarrett@nist.gov, shamith.payagala@nist.gov, afr@nist.gov).

This article has been accepted for publication in a future issue of this journal, but has not been fully edited. Content may change prior to final publication. Citation information: DOI 10.1109/TIM.2019.2941036, IEEE Transactions on Instrumentation and Measurement

Here, R_a and R_b can be included in leakage resistances, R_{LX1} and R_{LX2}, shown later in Figure 2, because they are connected to the case ground (GND) of the unknown resistor R_X and also to the system GND. Thus, the leakage resistances do not have significant influence on high resistance measurements using the various measurement methods described in the next section. By the Y-Δ transformations shown in Figure 1 and equation (1), 1 PΩ, 10 PΩ, and 100 PΩ resistances were generated, as summarized in Table I.

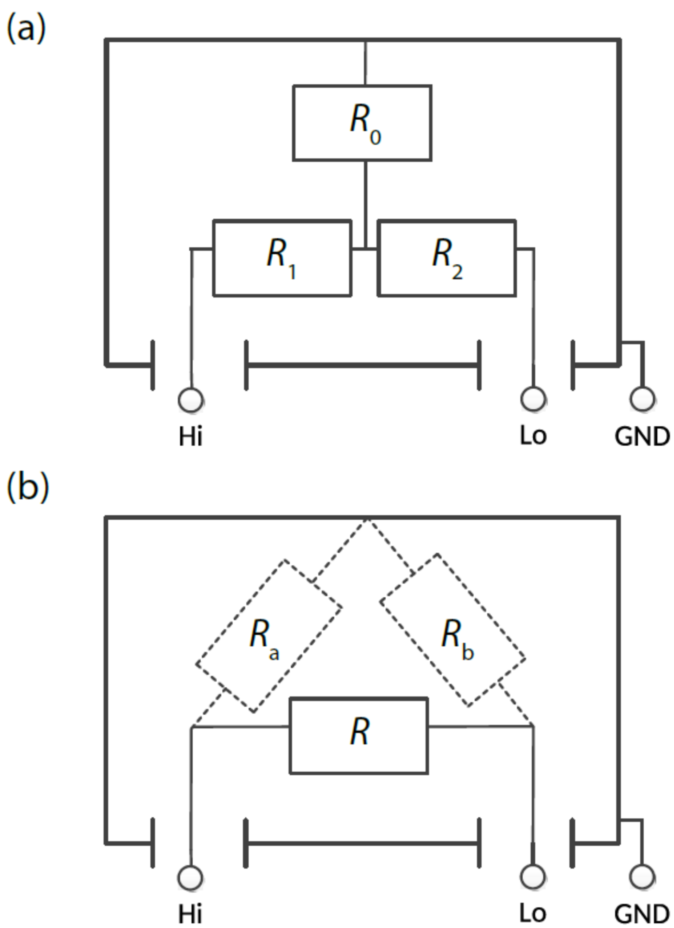

Fig. 1. The Y-Δ transformation for 1 PΩ, 10 PΩ, and 100 PΩ resistances. (a) Building a T-network with well-known standard resistors R_0, R_1, and R_2 can mathematically be transformed into the configuration shown in (b). (b) The post-transform effective circuit, where R is a much larger desired resistance value and R_a and R_b are negligibly small resistances.

TABLE I
1 PΩ, 10 PΩ, AND 100 PΩ RESISTANCES MADE BY Y-Δ TRANSFORMATIONS

Wye network (R_1–R_2–R_0)	R (PΩ) (nominal)	R_a (TΩ)	R_b (TΩ)
1 TΩ–1 TΩ–1 GΩ (A)	1	1	1
100 GΩ–100 GΩ–10 MΩ (B)	1	0.1	0.1
10 GΩ–10 GΩ–100 kΩ (C)	1	0.01	0.01
1 GΩ–1 GΩ–1 kΩ (D)	1	0.001	0.001
10 GΩ–10 GΩ–10 kΩ (E)	10	0.01	0.01
100 GΩ–100 GΩ–100 kΩ (F)	100	0.1	0.1

B. Uncertainty Calculation for Wye-Delta Networks

By the law of propagation of uncertainty, according to the ISO GUM Guide [19], the uncertainty for 1 PΩ, 10 PΩ, and 100 PΩ resistances calculated from equation (1) was derived as shown in equation (B2) of the Appendix. Table II shows the uncertainty calculated by putting NIST resistance standards into equation (B2) when those resistors are used as T-network elements, with lead resistances on the order of 6 mΩ. Lead resistances only need consideration in the case of the 1 kΩ resistor R_0.

TABLE II
CALCULATED UNCERTAINTY FOR 1 PΩ, 10 PΩ, AND 100 PΩ RESISTANCES

	R_1	R_2	R_0	R
Nominal Resistance	1 TΩ	1 TΩ	1 GΩ	1 PΩ
Actual Resistance	1.014 TΩ	0.992 TΩ	1.000 GΩ	1.008 PΩ
Uncertainty (σ)	5.00×10^7 Ω	5.00×10^7 Ω	5.00×10^3 Ω	7.118×10^{-5} PΩ
Nominal Resistance	100 GΩ	100 GΩ	10 MΩ	1 PΩ
Actual Resistance	0.999 GΩ	0.998 GΩ	10.000 MΩ	0.997 PΩ
Uncertainty (σ)	10^6 Ω	10^6 Ω	15 Ω	1.420×10^{-5} PΩ
Nominal Resistance	10 GΩ	10 GΩ	100 kΩ	1 PΩ
Actual Resistance	9.999 GΩ	10.042 GΩ	100.001 kΩ	1.004 PΩ
Uncertainty (σ)	10^5 Ω	10^5 Ω	4.000×10^{-2} Ω	1.418×10^{-5} PΩ
Nominal Resistance	1 GΩ	1 GΩ	1 kΩ	1 PΩ
Actual Resistance	1.000 GΩ	1.000 GΩ	1.000 kΩ	1.000 PΩ
Uncertainty (σ)	5.00×10^3 Ω	5.00×10^3 Ω	10^{-4} Ω	7.072×10^{-6} PΩ
Nominal Resistance	10 GΩ	10 GΩ	10 kΩ	10 PΩ
Actual Resistance	9.999 GΩ	10.042 GΩ	10.000 kΩ	10.042 PΩ
Uncertainty (σ)	10^5 Ω	10^5 Ω	10^{-3} Ω	1.417×10^{-4} PΩ
Nominal Resistance	100 GΩ	100 GΩ	100 kΩ	100 PΩ
Actual Resistance	99.871 GΩ	99.762 GΩ	100.001 kΩ	99.633 PΩ
Uncertainty (σ)	10^6 Ω	10^6 Ω	4.0000×10^{-2} Ω	1.412×10^{-3} PΩ

III. MEASUREMENT METHODS AND SETUP

A. Potentiometric Measurement Systems

While the basics of potentiometry can be summarized in the literature for measurements up to 1 TΩ resistance [20], modifications of this concept are needed to successfully measure 1 PΩ to 100 PΩ resistances. All versions of this first method are illustrated in Figure 2. As in Figure 2 (a), if a stable

DC voltage (V) is applied to a reference resistance (R_{S1}) and an unknown high resistance (R_X) is assembled using a Y-Δ transformations (T-network), the unknown resistance R_X can be determined by:

$$\frac{R_X}{R_{S1}} = \frac{V}{V_{S1}} - 1 \tag{2}$$

It should be noted, as done in [20], that this setup containing one voltage source and one voltmeter (VSVM) does not require an auxiliary shielding mechanism. So, in practice, measurements can rely solely on the stability of the voltage source while ignoring the effects of leakage between R_X and R_{s1}. And though accurate measurements can be made using this method, depending on the application, further corrections may be warranted.

The additional corrections can be applied using the leakage-cancelling modification of the VSVM method (LC-VSVM), as shown in Figure 2 (b). The leakage resistance R_L ($R_L^{-1} = R_{LX1}^{-1} + R_{LX2}^{-1} + R_{LS1}^{-1} + R_{DMM,input}^{-1}$) has a direct effect on measurements and can be reduced by both requiring an auxiliary shielding mechanism and by approximating R_L with a dummy resistor measurement (see [20]).

The potentiometric measurement system in Figure 2 (c) consists of one stable voltage source, one voltmeter, and an electromagnetic shielding enclosure (LCPM). It has one unknown resistance and two reference resistances. The advantage of this method over the previous two methods is mainly in its capacity to determine leakage resistances in the circuit of interest. In other words, measuring a dummy resistor to determine (and thus cancel R_L) is no longer necessary [20]. Additionally, if both are nominally the same value, an auxiliary shielding system is no longer required to obtain measurements where leakage resistances have been considered.

All cables used for the system are coaxially shielded and have British Post Office (BPO) terminals. For the experiment, 100 V and 500 V is applied from a voltage calibrator (Fluke 5720A) to the entire circuit, which includes an unknown resistance and two 10 GΩ NIST-made reference resistors [21], the latter of which were used to increase measurement sensitivity and remove leakage effects. More will be said on leakage resistances later in this section.

All resistors were calibrated with traceability to the NIST quantized Hall resistance (QHR) standard with corresponding resistance bridges. DC voltages of 1 mV, 0.1 mV, and 0.05 mV were measured across the 10 GΩ resistances and measured using a digital electrometer (Keithley 6430A) with 6-digit resolution, bias current of 0.1 fA, and input impedance greater than 10 PΩ. The high input impedance of the electrometer made it a better choice than an 8.5-digit digital voltmeter that has a typical input resistance of 10 GΩ. Measurements were made under laboratory conditions of 23.0 °C ± 0.3 °C and 40 % ± 5 % relative humidity. A single measurement displays an average value obtained by positive and negative polarities within about 1 hr.

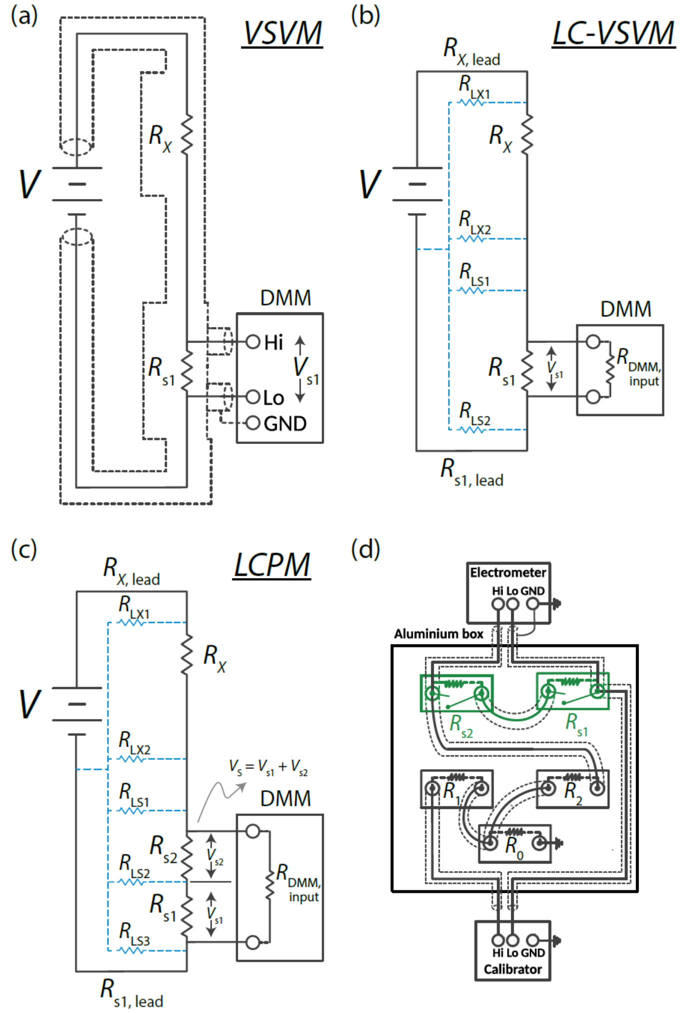

Fig. 2. Simplified diagram for various potentiometric methods. (a) This setup has one voltage source and one voltmeter (VSVM) and the DC voltage (V_{S1}) across R_{S1} is measured using an electrometer with very high input resistance. R_X is the unknown resistance. The dotted line represents optional auxiliary shielding that is required for (b) (not shown for other methods for visual clarity). (b) This setup is a leakage-cancelling modification (LC-VSVM) of the first and includes leakage resistances, a DMM input resistance, and lead wire resistances. Subscripts containing *X*, *L*, or *S* are referring to the unknown quantity, leakage quantity, and standard quantity, respectively. (c) Most lead resistances and other circuit elements are similar to (b) with the exception of an added standard resistor, R_{S2}, as well as its corresponding leakage resistance and voltage. It is also known as the leakage-cancelling potentiometric method (LCPM). (d) Systematic diagram for all potentiometric resistance measurements. R_X is a T-network made of three standard resistors (R_1, R_2 and R_0) and the reference resistors in green (R_{s1} and R_{s2}) are shown above the standard resistors. The switches shown in parallel with R_{s1} and R_{s2} are able to short either resistor, as needed for the LC-VSVM measurement.

R_L is typically 10 TΩ or higher (R_L>>R_{s1}), signifying that the leakage effect is negligible, as confirmed in previous work [20]. However, 1 PΩ, 10 PΩ and 100 PΩ resistances, made using T-networks, have relatively small resistor elements, R_a and R_b, as shown in Table I. R_a and R_b are represented by R_{LX1} and R_{LX2}, respectively. Thus, as shown in Figure 2 (b), the leakage resistance R_L includes R_a, R_b, and insulation resistances of the system circuit and reference resistors. The R_{S1} term of equation (2) can thus be replaced by R_b and R_a, allowing R_X to be successfully determined by equation (2) since R_b and R_a are

This article has been accepted for publication in a future issue of this journal, but has not been fully edited. Content may change prior to final publication. Citation information: DOI 10.1109/TIM.2019.2941036, IEEE Transactions on Instrumentation and Measurement

known. For Figure 2 (c), another modification can be made to cancel leakage resistances using another reference resistance R_{S2} with nominally-equal resistance as R_{S1}, to within a linear approximation [19]. That is, one can measure V_{S1} by short-circuiting R_{S2} and measuring V_S across R_{S1} and R_{S2}. Then, the following two equations may be used:

$$\frac{V}{V_S} = 1 + \frac{R_X}{R_L} + \frac{R_X \cdot (R_{S1} + R_{LS2})}{R_{S1} \cdot R_{LS2} + R_{S2} \cdot (R_{S1} + R_{LS2})} \quad (3)$$

$$\frac{V}{V_{S1}} = 1 + \frac{R_X}{R_L} + \frac{R_X}{R_{LS2}} + \frac{R_X}{R_{S1}} \quad (4)$$

Considering that R_{LS2} is about 100 TΩ or higher, R_X can be approximated by subtracting equations (3) and (4) as such [20]:

$$\frac{V}{V_{S1}} - \frac{V}{V_S} \approx R_X \cdot \left\{\frac{1}{R_{S1}} - \frac{1}{(R_{S1} + R_{S2})}\right\} \quad (5)$$

From equation (5), the system insulation is supposed to measure about 100 TΩ, so it cannot be neglected in measuring resistances higher than 1 TΩ. Thankfully, the methods shown in Figure 2 alleviates this condition, thereby allowing us to measure arbitrarily high resistances without system leakage effects. To accomplish this, measure V_{S2} by short-circuiting R_{S1} in addition to the LC-VSVM shown in Figure 2 (b), equation (3) and (4). We may now establish:

$$\frac{V}{V_{S2}} = 1 + \frac{R_X}{R_L} + \frac{R_X}{R_{S2}} \quad (6)$$

From equation (3), (4) and (6), the unknown resistance R_X is determined by:

$$R_X = R_{S2} \cdot \left(\frac{V}{V_{S2}} - \frac{V}{V_S}\right) \pm R_{S2} \cdot \sqrt{\left(\frac{V}{V_{S2}} - \frac{V}{V_S}\right) \cdot \left(\frac{V}{V_{S1}} - \frac{V}{V_S}\right)} \quad (7)$$

Either sign may be taken with the relative magnitude of R_{S1} and R_{S2}. Equation (7) is independent of leakage resistances R_L and R_{LS2}. For more information, a combined standard uncertainty for equation (7) is derived in the Appendix.

A systematic diagram for the 1 PΩ, 10 PΩ, and 100 PΩ resistance measurements using VSVM, LC-VSVM, and LCPM sub-methods is shown in Figure 2 (d). Three standard resistors (R_1, R_2 and R_0) comprise an unknown resistance (R_X), which takes the form of a T-network on the bottom side of the aluminum box. The reference resistors (R_{s1} and R_{s2}) are shown on the top side of the aluminum box. Solid lines represent connection of the coaxial terminations of the standard resistors and the dotted lines represent the shields of the coaxial cables used to interconnect the standard resistors shields and cases.

B. The Dual Source Bridge and Teraohmmeter

To further validate predictions obtained with the Y-Δ transformations, we also performed measurements using a DSB and a commercial TM. Figure 3 (a) shows a DSB that is a modified Wheatstone bridge that has been implemented at various NMIs [7, 8, 14, 23]. On one arm, a voltage V_1 is applied across an unknown resistance R_X, while on the second arm, a voltage V_2 is applied with opposite polarity across a reference resistor R_S. The voltage is then modified until the detector (labelled D) reads a null signal. One of the significant advantages of using a DSB is that very low uncertainties can be achieved due to the proper and facile calibration of the applied voltages. Furthermore, leakage effects are negligible since the sensitive bridge point voltage is balanced to zero. For these higher resistance values, only current null-detection is recommended because R_S becomes comparable to the input impedance of typical nanovoltmeters. Accurate measurements of T-networks using a DSB require the low terminal of R_2 to be at the same potential as the low terminal of R_0. Major sources of uncertainty with this DSB approach include the calibration of the voltage sources, noise, offset voltages, and the reference resistors R_S. Another source of error could be the input burden voltage of the null detector since, with the T-network effectively forming a voltage divider, the current across R_2 is in a similar range as the burden voltage of typical electrometers.

Another way of determining high resistances, even if they are effective resistances, is with the TM, whose diagram is shown in Figure 3 (b). For this method, a measurement voltage V_S is applied to the unknown effective resistance (represented by T-networks) R_X. The resulting current is then integrated by a high-input impedance operational amplifier with a feedback element of capacitance C, with the output of the integrator providing a linearly ramping voltage. A voltage comparator and timer are subsequently used to measure the time required for the integrator output to undergo a change defined by the voltage comparator limits. The value of the unknown resistance R_X can then be calculated as demonstrated in Ref. [14].

This article has been accepted for publication in a future issue of this journal, but has not been fully edited. Content may change prior to final publication. Citation information: DOI 10.1109/TIM.2019.2941036, IEEE Transactions on Instrumentation and Measurement

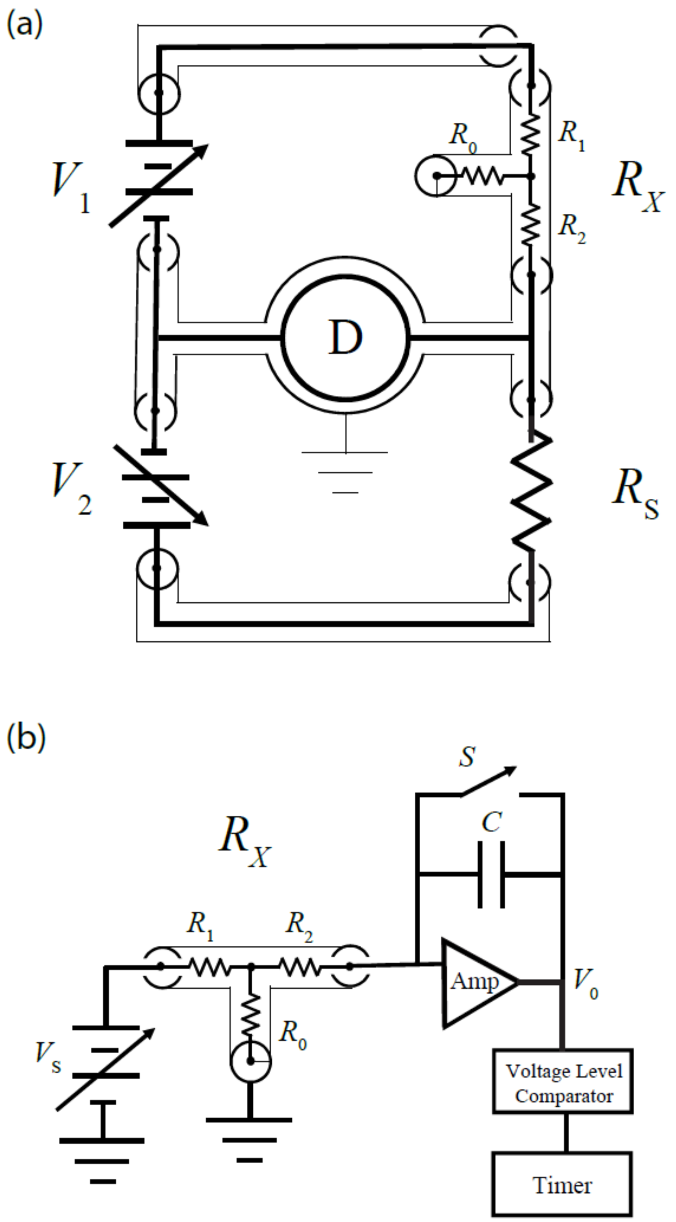

Fig. 3. (a) Schematic diagram is shown for the NIST DSB, where R_S is the known standard resistance, D is the null detector, and the two voltage sources each occupy of one the voltage arms of the bridge. (b) The diagram for the commercially-obtained TM provides an overview of the current integration technique as required for the measurement of high resistances. In both cases, the unknown standard resistance R_X is replaced by the T-network configuration, as prescribed by corresponding Y-Δ transformations.

TABLE III
RESULTS FOR 1 PΩ, 10 PΩ, AND 100 PΩ RESISTANCES

T-network (A) 1 TΩ – 1 TΩ – 1 GΩ	Voltage	Resistance (PΩ)	Expanded uncertainty (%, k=2)
VSVM	100 V	1.008	0.4
LC-VSVM	100 V	1.003	1.0
LCPM	100 V	1.007	1.2
DSB	250 V	1.008	0.5
DSB	500 V	1.008	0.3
DSB	750 V	1.008	0.3
TM	200 V	1.002	2.5
TM	500 V	1.010	2.5
Calculation	-	1.006	<0.05
T-network (B) 100 GΩ – 100 GΩ – 10 MΩ	**Voltage**	**Resistance (PΩ)**	**Expanded uncertainty (%, k=2)**
VSVM	100 V	0.997	0.4
LC-VSVM	100 V	0.993	1.2
LCPM	100 V	1.002	1.4
DSB	250 V	0.998	0.6
DSB	500 V	0.996	0.4
DSB	750 V	0.997	0.3
TM	500 V	0.999	2.5
Calculation	-	0.996	<0.01
T-network (C) 10 GΩ – 10 GΩ – 100 kΩ	**Voltage**	**Resistance (PΩ)**	**Expanded uncertainty (%, k=2)**
VSVM	100 V	1.004	0.4
LC-VSVM	100 V	1.004	1.0
LCPM	100 V	1.003	1.0
TM	200 V	1.005	2.5
TM	500 V	1.009	2.5
Calculation	-	1.004	<0.005
T-network (D) 1 GΩ – 1 GΩ – 1 kΩ	**Voltage**	**Resistance (PΩ)**	**Expanded uncertainty (%, k=2)**
VSVM	100 V	1.004	1.4
LC-VSVM	100 V	0.998	3.6
LCPM	100 V	0.995	4.8
DSB	200 V	1.013	4.8
TM	200 V	1.061	2.5
Calculation	-	1.000	<0.001
T-network (E) 10 GΩ – 10 GΩ – 10 kΩ	**Voltage**	**Resistance (PΩ)**	**Expanded uncertainty (%, k=2)**
VSVM	100 V	10.07	2.8
VSVM	500 V	10.02	2.8
LC-VSVM	100 V	9.98	4.8
LCPM	100 V	10.69	5.6
DSB	500 V	9.89	2.2
TM	1000 V	9.74	30
Calculation	-	10.04	<0.005
T-network (F) 100 GΩ – 100 GΩ – 100 kΩ	**Voltage**	**Resistance (PΩ)**	**Expanded uncertainty (%, k=2)**
VSVM	500 V	99.9	4.4
LC-VSVM	500 V	100.3	6.8
LCPM	500 V	98.6	10.2
Calculation	-	99.6	<0.01

IV. MEASUREMENT RESULTS AND DISCUSSION

A. 1 PΩ, 10 PΩ, and 100 PΩ Resistances

T-networks were used to generate six effective resistances, of which four were 1 PΩ, one was 10 PΩ, and one was 100 PΩ. Having done the measurements with one of the three aforementioned methods (potentiometric, DSB, and TM), the results were able to be compared with calculated values. These results are shown in Table III and are graphically illustrated in Figures 4 and 5.

This article has been accepted for publication in a future issue of this journal, but has not been fully edited. Content may change prior to final publication. Citation information: DOI 10.1109/TIM.2019.2941036, IEEE Transactions on Instrumentation and Measurement

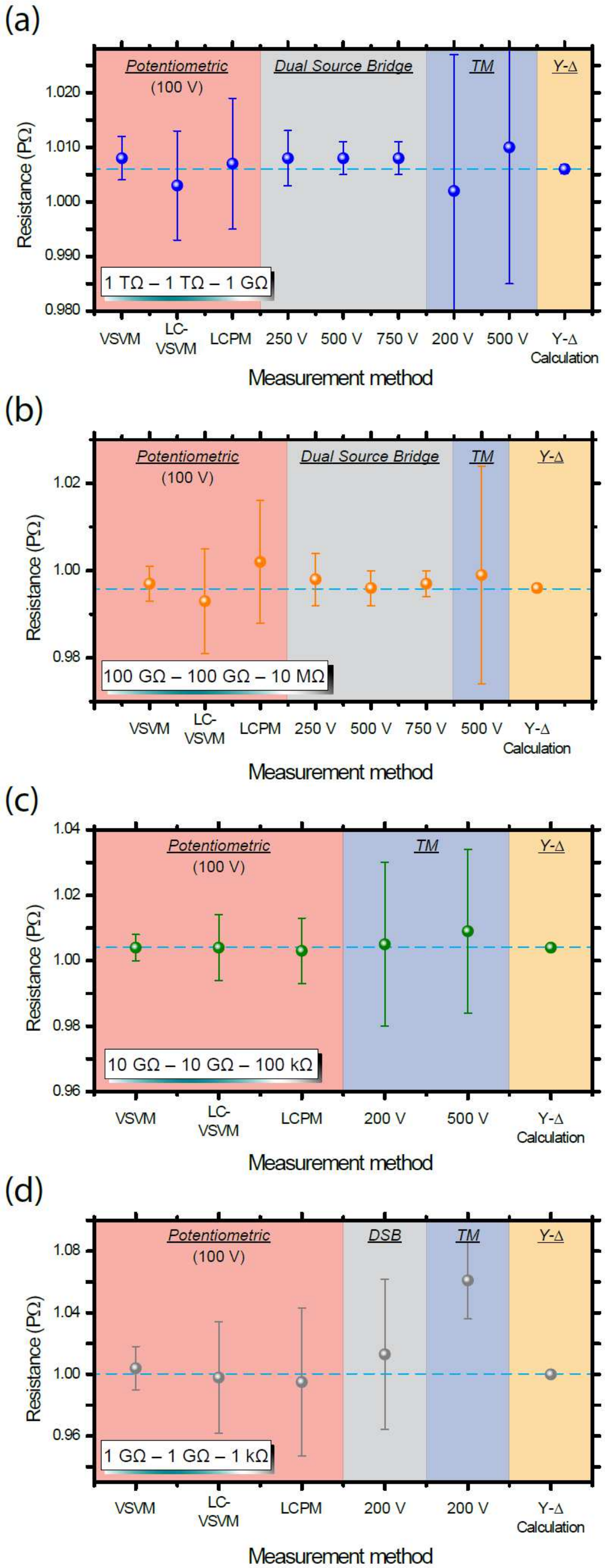

Fig. 4. Each 1 PΩ resistance is generated by a T-network and measured with three experimental methods (with sub-methods listed for each in some cases) and one theoretical calculation. Potentiometric, DSB, and TM methods are within the red, gray, and blue regions, respectively whereas the Y-Δ calculations are within gold regions. The following T-networks are represented: (a) 1 TΩ – 1 TΩ – 1 GΩ (b) 100 GΩ – 100 GΩ – 10 MΩ (c) 10 GΩ – 10 GΩ – 100 kΩ (d) 1 GΩ – 1 GΩ – 1 kΩ. All error bars correspond to the expanded uncertainties (k = 2).

Figure 4 focuses on the 1 PΩ generated resistance, whose T-network components are designated in the format: $R_1 – R_2 – R_0$. For three of the four networks, the four methods are used to validate the measurement of 1 PΩ (the DSB was not used for the 10 GΩ – 10 GΩ – 100 kΩ T-network in Figure 4 (c)). For some measurements, different voltages were used to provide a basis of comparison for the accuracy within the one measurement type. The error bars correspond to the expanded uncertainties (k = 2). Having several configurations allowed for the assessment of the versatility of T-networks, namely in their increased compatibility with some of the measurement methods over others. For instance, it may be advantageous to customize a configuration based on the equipment intended for use, such as using the DSB for configurations like Figure 4 (a) and (b).

Figure 5 focuses on both 10 PΩ and 100 PΩ generated resistances, and like Figure 5, the T-network components are designated in the format: $R_1 – R_2 – R_0$. Though four methods were used to validate the measurement of 10 PΩ, only two methods were used to validate the 100 PΩ resistance. The error bars correspond to the expanded uncertainties (k = 2).

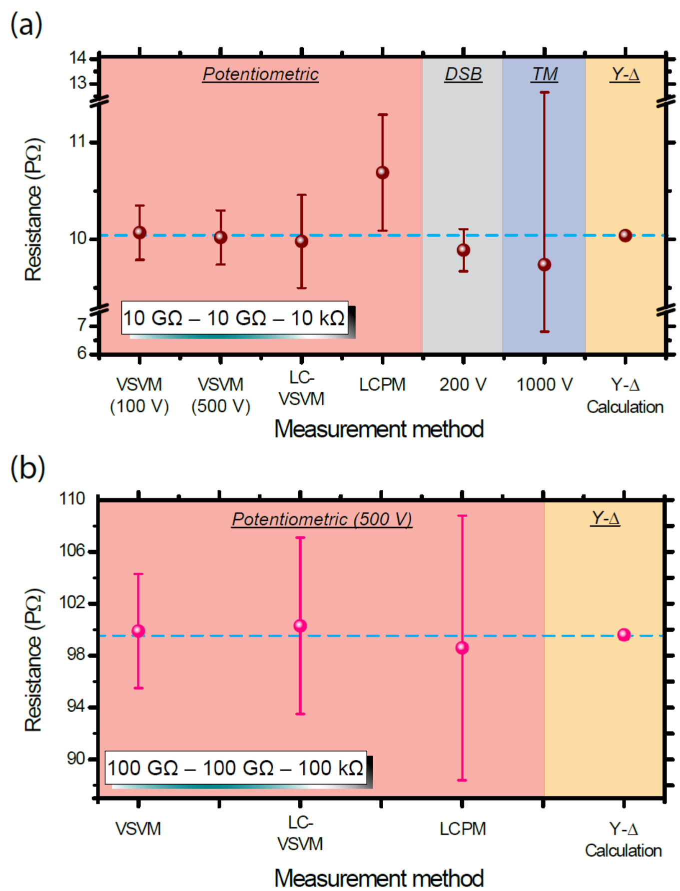

Fig. 5. Both 10 PΩ and 100 PΩ resistances are generated by T-networks and measured with potentiometric, DSB, and TM methods (shown as red, gray, and blue regions, respectively). Corresponding Y-Δ calculations are within gold regions. The following T-networks are represented: (a) 10 GΩ – 10 GΩ – 10 kΩ (b) 100 GΩ – 100 GΩ – 100 kΩ. All error bars correspond to the expanded uncertainties (k = 2).

This article has been accepted for publication in a future issue of this journal, but has not been fully edited. Content may change prior to final publication. Citation information: DOI 10.1109/TIM.2019.2941036, IEEE Transactions on Instrumentation and Measurement

B. *Voltage Effects*

The voltage effects for 1 PΩ and 10 PΩ resistances were investigated using the VSVM and two 10 GΩ reference resistances, with the results shown in Table IV. Voltage effects were not determined for two of the networks. The first T-network, 1 GΩ – 1 GΩ – 1 kΩ, comprised one form of 1 PΩ resistance and its voltage effects were not investigated to avoid damaging the 1 kΩ resistor. For the 100 PΩ resistance (100 GΩ – 100 GΩ – 100 kΩ T-network), the effects were not investigated because measurement sensitivity was generally too low at 100 V. From these measurements, the voltage effects were shown to be about 0.03 % for the 1 PΩ resistance standards and about 0.1 % for the 10 PΩ resistance standards. Thus, voltage effects on the T-network resistance standards are negligible.

TABLE IV
VOLTAGE EFFECTS FOR 1 PΩ AND 10 PΩ RESISTANCES

T-network	Voltage	Value (PΩ)
1 TΩ – 1 TΩ – 1 GΩ	100 V	1.0098
	500 V	1.0086
100 GΩ – 100 GΩ – 10 MΩ	100 V	0.9972
	500 V	0.9985
10 GΩ – 10 GΩ – 100 kΩ	100 V	1.0035
	500 V	1.0037
10 GΩ – 10 GΩ – 10 kΩ	100 V	10.065
	500 V	10.019

C. *Uncertainty Estimation*

The combined standard uncertainties for the VSVM, LC-VSVM, and LCPM which is given by the law of propagation of uncertainty according to ISO GUM Guide [19] can be derived from equation (2), (5) and (7). The results for the former two methods are given by:

$$\frac{u_{\mathrm{C}}{}^2(R_X)}{R_X{}^2} = \frac{u^2(R_{\mathrm{S1}})}{R_{\mathrm{S1}}{}^2} + \frac{u^2(V)}{V^2} + \frac{u^2(V_{\mathrm{S1}})}{V_{\mathrm{S1}}{}^2} \tag{8}$$

$$\frac{u_{\mathrm{C}}{}^2(R_X)}{R_X{}^2} = \frac{u^2(V)}{V^2} + \frac{u^2(V_{\mathrm{S1}})}{V_{\mathrm{S1}}{}^2} + \frac{u^2(V_{\mathrm{S}})}{V_{\mathrm{S}}{}^2} + 2.25\frac{u^2(R_{\mathrm{S1}})}{R_{\mathrm{S1}}{}^2} + 0.25\frac{u^2(R_{\mathrm{S2}})}{R_{\mathrm{S2}}{}^2} \tag{9}$$

Where equation (9) applies for $R_x/R_{s1} \geq 10$. The derived result for the LCPM is shown in appendix A and is expressed by:

$$\frac{u^2(R_X)}{R_X{}^2} \approx \frac{u^2(R_{\mathrm{S2}})}{R_{\mathrm{S2}}{}^2} + \frac{u^2(V)}{V^2} + \frac{u^2(V_{\mathrm{S}})}{V_{\mathrm{S}}{}^2} + \frac{1}{4}\frac{u^2(V_{\mathrm{S1}})}{V_{\mathrm{S1}}{}^2} + \frac{9}{4}\frac{u^2(V_{\mathrm{S2}})}{V_{\mathrm{S2}}{}^2} \tag{10}$$

TABLE V
UNCERTAINTY BUDGETS FOR 1 PΩ, 10 PΩ, AND 100 PΩ RESISTANCE MEASUREMENTS (POTENTIOMETRIC METHOD)

Uncertainty source	Standard uncertainty (%)					
	1 PΩ	1 PΩ	1 PΩ	1 PΩ	10 PΩ	100 PΩ
	A	B	C	D	E	F
Voltage source (100 V, 500 V)	0.0005	0.0005	0.0005	0.0005	0.0005	0.0005
Calibration	0.0005	0.0005	0.0005	0.0005	0.0005	0.0005
Stability (short-term)	0.0002	0.0002	0.0002	0.0002	0.0002	0.0002
Voltmeter (V_{S1})	0.07	0.07	0.11	0.7	1.3	2.1 (500V)
Calibration (short-term)	0.06	0.06	0.1	0.6	1.2	2
Resolution	0.03	0.03	0.05	0.3	0.6	0.6
Reference standards (R_{S1}, 10 GΩ)	0.0014	0.0014	0.0014	0.0014	0.0014	0.0014
Calibration	0.001	0.001	0.001	0.001	0.001	0.001
Temperature	0.0005	0.0005	0.0005	0.0005	0.0005	0.0005
Voltage	0.0006	0.0006	0.0006	0.0006	0.0006	0.0006
Stability (3 month)	0.0006	0.0006	0.0006	0.0006	0.0006	0.0006
Leakage effect	<0.1	<0.1	<0.1	<0.1	<0.1	<0.1
Repeatability (100 V)	0.1	0.1	0.1	0.1	0.6	0.8 (500V)
Combined Standard Uncertainty (VSVM)	**0.2**	**0.2**	**0.2**	**0.7**	**1.4**	**2.2**
Voltmeter	0.04	0.04	0.09	0.7	0.09	1.2 (500V)
Calibration (short-term)	0.03	0.03	0.08	0.6	0.08	1
Resolution	0.02	0.02	0.04	0.3	0.04	0.3
Reference standards (R_{s2}, 10 GΩ)	0.0004	0.0004	0.0004	0.0004	0.0004	0.0004
Calibration	0.0003	0.0003	0.0003	0.0003	0.0003	0.0003
Temperature	0.0002	0.0002	0.0002	0.0002	0.0002	0.0002
Voltage	0.0002	0.0002	0.0002	0.0002	0.0002	0.0002
Stability (3 month)	0.0002	0.0002	0.0002	0.0002	0.0002	0.0002
Leakage effect	<0.1	<0.1	<0.1	<0.1	<0.1	<0.1
Repeatability (100 V)	0.4	0.6	0.4	1.5	1.7	2.3 (500V)
Combined Standard Uncertainty (LC-VSVM)	**0.5**	**0.6**	**0.5**	**1.8**	**2.4**	**3.4**
Voltmeter	0.07	0.07	0.11	0.07	1.3	2.1 (500V)
Calibration (short-term)	0.06	0.06	0.1	0.06	1.2	2
Resolution	0.03	0.03	0.05	0.03	0.6	0.6
Leakage effect	<0.1	<0.1	<0.1	<0.1	<0.1	<0.1
Repeatability (100 V)	0.2	0.3	0.2	1.3	0.7	2.7 (500V)
Combined Standard Uncertainty (LCPM)	**0.6**	**0.7**	**0.5**	**2.4**	**2.8**	**5.1**

Equation (10) applies for $R_x/R_{s1} \geq 1000$. Correlations among V_S, V_{S1} and V_{S2} in equation (9) and (10) were estimated by the

ISO GUM guide and were negligible. The measurement uncertainty budgets for the potentiometric variants, namely VSVM, LC-VSVM, and LCPM, are shown in Table V and the uncertainty of TM was estimated by its specification. All three resistances (1 PΩ, 10 PΩ, and 100 PΩ) are shown on this table. It should be noted that the labels A, B, C, D, E, and F correspond to the same T-networks listed in Table I and are marked similarly below.

An example uncertainty budget for the dual source bridge [24] measurements are shown in Table VI. The dual source bridge used a 10 TΩ standard resistor as the standard for both the 1 PΩ (1 TΩ – 1 TΩ – 1 GΩ T-network) and 10 PΩ measurements of the T-networks and the bridge ratios were 1:100 and 1:1000, respectively. Measurements of the 1 PΩ resistance (1 GΩ – 1 GΩ – 1 kΩ T-network) yielded higher type A uncertainties than shown in Table VI due to decreased detector resolution, as discussed below.

TABLE VI
UNCERTAINTY BUDGET FOR 1 PΩ AND 10 PΩ DSB RESISTANCE MEASUREMENTS (10^{-6} Ω/Ω)

Nominal Resistance	1 PΩ	10 PΩ
Type A Uncertainty	1175	9761
Type B Uncertainties		
10 TΩ Standard Uncertainty	337	337
V_1 Voltage Source (1 year)	3.5	3.5
V_2 Voltage Source (1 year)	2.5	2.5
Detector Resolution	500	5000
Leakage	10	10
Stability of 10 TΩ Standard (regression)	80	80
Voltage Coefficient of 10 TΩ (0.11 × 10^{-6}/V)	33	33
Temperature Coefficient of 10 TΩ (200 × 10^{-6}/°C)	10	10
Type B Total	609	5012
Combined Standard Uncertainty	1324	10973
Expanded Uncertainty (k=2)	2648	21946
Expanded Uncertainty (k=2) (%)	**0.26**	**2.2**

D. Discussion

When measuring a 1 PΩ standard resistor formed by the 1 GΩ – 1 GΩ – 1 kΩ T-network (D), R_a and R_b of the Y-Δ network corresponds to the 1 GΩ resistance standard, which makes a parallel connection with the 10 GΩ reference resistance standards. This makes the measurement ratio not 1 PΩ to 10 GΩ, but 1 PΩ to 1 GΩ. As a result, the measurement resolution decreased, and the uncertainty was shown to be larger than that of other wye networks of 1 PΩ as shown in Table IV. The decreased resistance of R_a and R_b in the Y-Δ network can also give some errors on 1 PΩ measurements of the 1 GΩ – 1 GΩ – 1 kΩ T-network.

Four different 1 PΩ resistance configurations were selected because of the varying uncertainties obtainable with low values of R_0. An exact value of R_0, which includes lead resistances to the measurement system ground, is needed and leakage effects (for instance, R_{LS2}) must be considered (in our cases, via R_1 and R_2). As stated earlier, the data from different configurations reveal the extent of compatibility with some measurement methods compared with others. Furthermore, using extreme resistances, both high (1 TΩ) and low (1 kΩ), for the highest R_1 and R_2 resistances and the lowest R_0 resistances, respectively, resulted in a demonstration of the approximate upper and lower limits of the techniques for 1 PΩ.

One of the advantages of LCPM, compared to the VSVM and LC-VSVM techniques, is that LCPM measures a high resistance standard while considering effects from leakage, making the method the most rigorous of the three. Higher resolution than that of VSVM is needed for LC-VSVM and LCPM when reference standard resistors are of similar nominal value because the difference of the voltages measured across the two reference standard resistors is used for LC-VSVM and LCPM. Therefore, if the reference standard resistors have different resistance values, like 10 GΩ and 20 GΩ, simple and accurate measurements can be made by the LC-VSVM and LCPM methods as is done with the VSVM. For measurement of 100 PΩ resistance standards, the measurement resolution can be improved by using 1 TΩ standard resistors for the references, rather than the 10 GΩ resistance standards used for references in the experiment.

A second advantage of the LCPM method introduced here includes its capacity to use ratios beyond the usual one-to-one or ten-to-one ratio between reference and unknown standard. Instead, large ratios, such as one-thousand-to-one ratio or higher ratios can be used, resulting in the accurate measurement of very high resistance standards, such as 1 PΩ or higher, using much smaller reference standard resistors. Because much smaller reference standard resistors are used in this method, the leakage effect can be minimized or completely eliminated. Thirdly, the inherent configuration of the T-network enables the accurate measurement of insulation resistances of materials, cables, and measurement systems. Furthermore, the corresponding voltage effects for high resistances can be easily determined since the methods use, as references, standard resistors of lower nominal value and negligible voltage effects.

The VSVM and LC-VSVM were previously used for 10 kΩ to 1 TΩ resistance measurements [19]. For other combinations of resistors in T-networks, it may be possible to achieve EΩ resistances, but as seen in Figures 4 and 5, the methods would be limited to potentiometric ones. Even then, uncertainties may increase by additional orders of magnitude, rendering the measurements questionable for metrology, at best. The potentiometric method along with the DSB and TM methods have now been demonstrated in the 1 PΩ to 100 PΩ range for resistance measurements. In summary, these three methods can be selectively used according to the needs of the researcher.

V. CONCLUSION

Several methods for measuring high resistances are demonstrated here: potentiometry, dual source bridge measurements, and use of a teraohmmeter. All results have also been compared to calculated resistances using the Y-Δ transformations. These methods were used to measure four 1 PΩ resistances, one 10 PΩ resistance, and one 100 PΩ resistance. All comparisons have good agreement within their uncertainties, typically within 1 % of the theoretical values. The

This article has been accepted for publication in a future issue of this journal, but has not been fully edited. Content may change prior to final publication. Citation information: DOI 10.1109/TIM.2019.2941036, IEEE Transactions on Instrumentation and Measurement

measurement uncertainties for the three methods were estimated to be 0.4 % to 1.2 % for 1 PΩ, 2.8 % to 5.6 % for 10 PΩ, and 4.4 % to 10.2 % for 100 PΩ. Insulation resistances and voltage effects of materials, cables, and measurement systems may now be simply and accurately measured using these methods.

APPENDIX

A. Derivation of Combined Standard Uncertainty for Potentiometric Method Variants

Supposed that $\mathrm{V_{S2}} = \mathrm{V_{S1}} + \delta\mathrm{V}$ and $\delta\mathrm{V}/\mathrm{V_{S1,2}}$ is less than 1×10^{-3}, higher order terms following the first order term in the second term of equation (7) can be neglected (to within 1×10^{-6} uncertainty) and the second term can be expressed by:

$$\sqrt{\left(\frac{V}{V_{S2}}-\frac{V}{V_S}\right)\cdot\left(\frac{V}{V_{S1}}-\frac{V}{V_S}\right)} \approx \sqrt{\left(\frac{V}{V_{S1}}-\frac{V}{V_S}\right)^2\left\{1-\frac{1}{\left(\frac{V}{V_{S1}}-\frac{V}{V_S}\right)}\cdot\frac{V\cdot\delta V}{V_{S1}^2}\right\}} \tag{A1}$$

If the ratio of R_X to R_S is more than 1,000, taking a linear approximation is appropriate, leading to a simplified equation (within 2×10^{-6} uncertainty):

$$R_X = R_{S2}\left\{\left(\frac{V}{V_{S2}}-\frac{V}{V_S}\right)+\left(\frac{V}{V_{S1}}-\frac{V}{V_S}\right)-\frac{1}{2}\frac{V}{V_{S1}}\cdot\frac{\delta V}{V_{S1}}\right\} \tag{A2}$$

Or

$$R_X = R_{S2}\left\{\frac{V}{V_{S2}}-\frac{2V}{V_S}+\frac{V}{V_{S1}}\cdot\left(\frac{3}{2}-\frac{V_{S2}}{2V_{S1}}\right)\right\} \tag{A3}$$

Let us suppose that $V_{S2} = V_{S0}(1+\delta_{S2})$, $V_{S1} = V_{S0}(1+\delta_{S1})$, $V_S = nV_{S0}(1+\delta_S)$. Then, equation (A3) can be linearly approximated as:

$$R_X \approx R_{S2}\cdot\frac{V}{V_{S0}}\left\{\left(2-\frac{2}{n}\right)+\frac{2}{n}\cdot\delta_S-\frac{1}{2}\cdot\delta_{S1}-\frac{3}{2}\cdot\delta_{S2}\right\} = R_{S2}\cdot\frac{V}{V_{S0}}\cdot f(v) \tag{A4}$$

Then a combined standard uncertainty for f(v) is given by:

$$u^2\{f(v)\} = \frac{4}{n^2}u^2(\delta_S)+\frac{1}{4}u^2(\delta_{S1})+\frac{9}{4}u^2(\delta_{S2}) \tag{A5}$$

B. Derivation of Combined Standard Uncertainty for Y-Δ Transformations

By the law of propagation of uncertainty in the ISO Guide, the combined standard uncertainty of an unknown resistance R is given by:

$$u^2(R) = \left(\frac{\partial R}{\partial R_1}\right)^2\cdot u^2(R_1)+\left(\frac{\partial R}{\partial R_2}\right)^2\cdot u^2(R_2)+\left(\frac{\partial R}{\partial R_0}\right)^2\cdot u^2(R_0) \tag{B1}$$

In equation (B1), $\frac{\partial R}{\partial R_1} = \frac{R_2}{R_0}+1$, $\frac{\partial R}{\partial R_2} = \frac{R_1}{R_0}+1$ and $\frac{\partial R}{\partial R_0} = -\frac{R_1 \cdot R_2}{R_0{}^2}$.

The relative expression of equation (B1) is given by:

$$\begin{aligned}\frac{u^2(R)}{R^2} &= \frac{\left(\frac{R_2}{R_0}+1\right)^2\cdot u^2(R_1)}{\left\{R_1\cdot\left(\frac{R_2}{R_0}+1\right)+R_2\right\}^2}+\frac{\left(\frac{R_1}{R_0}+1\right)^2\cdot u^2(R_2)}{\left\{R_2\cdot\left(\frac{R_1}{R_0}+1\right)+R_1\right\}^2} \\ &\quad +\frac{\left(\frac{R_1\cdot R_2}{R_0{}^2}\right)^2\cdot u^2(R_0)}{\left(\frac{R_1\cdot R_2}{R_0}+R_1+R_2\right)^2} \\ &= \frac{u^2(R_1)}{R_1{}^2}\cdot\frac{\left(\frac{R_2}{R_0}+1\right)^2}{\left\{\left(\frac{R_2}{R_0}+1\right)+\frac{R_2}{R_1}\right\}^2}+\frac{u^2(R_2)}{R_2{}^2} \\ &\quad \cdot\frac{\left(\frac{R_1}{R_0}+1\right)^2}{\left\{\left(\frac{R_1}{R_0}+1\right)+\frac{R_1}{R_2}\right\}^2}+\frac{u^2(R_0)}{R_0{}^2}\cdot\frac{\left(\frac{R_1\cdot R_2}{R_0}\right)^2}{\left(\frac{R_1\cdot R_2}{R_0}+R_1+R_2\right)^2} \\ &\approx \frac{u^2(R_1)}{R_1{}^2}+\frac{u^2(R_2)}{R_2{}^2}+\frac{u^2(R_0)}{R_0{}^2}\end{aligned} \tag{B2}$$

This result is satisfied within a few 10^{-6} of uncertainty.

ACKNOWLEDGMENT

The authors would like to thank T. Larason, E. C. Benck, and A. D. Koffman for their assistance during the internal review process at NIST. This work was partly supported by the Korea Research Institute of Standards and Science under Grant # 14011001. Certain commercial equipment, instruments, or materials are identified in this paper to foster understanding. Such identification does not imply recommendation or endorsement by the National Institute of Standards and Technology or the United States Government, nor does it imply that the materials or equipment identified are necessarily the best available for the purpose.

REFERENCES

[1] CCEM.EM-K2 2002 Metrologia **39**. Tech. Suppl. 01001
[2] SIM.EM-K1-S6-K2 2009 Metrologia **46**. Tech. Suppl. 01001
[3] EURAMET.EM-K2 2010 Metrologia **47**. Tech. Suppl. 01006
[4] Final report on supplementary comparison EURAMET.EM-S32: Comparison of resistance standards at 1 TΩ and 100 TΩ 2013 Metrologia **50**. Tech. Suppl. 01008
[5] APMP.EM-K2 in progress
[6] S. H. Tsao, "An accurate, semiautomatic technique of measuring high resistances," *IEEE Trans. Instrum. Meas*., 16, 220-225, 1967.
[7] L. C.A. Henderson, "A new technique for the automatic measurement of high value resistors," *J. Phys. E: Sci. Instrum*., 20, 492-495, 1987.
[8] D. G. Jarrett, "Automated guarded bridge for calibration of multimegohm standard resistors from 10MΩ to 1 TΩ," *IEEE Trans. Instrum. Meas.,* 46, 325–328, 1997.
[9] D. G. Jarrett and M. E. Kraft, "10 TΩ and 100 TΩ Resistance Measurements at NIST," *X-Semetro Congress. Digest*, Sept. 25-27, 2013.
[10] G. Rietveld and J.H.N. van der Beek, "Automated High-Ohmic Resistance Bridge with Voltage and Current Null-detection," *IEEE Trans. Instr. Meas*., 62 1760-1765, 2013.
[11] F. Galliana, P.P. Capra, E. Gasparotto, "Metrological management of the high dc resistance scale at INRIM," *Measurement,* 42, 314-321, 2009.

This article has been accepted for publication in a future issue of this journal, but has not been fully edited. Content may change prior to final publication. Citation information: DOI 10.1109/TIM.2019.2941036, IEEE Transactions on Instrumentation and Measurement

[12] F. Galliana, P.P. Capra, E. Gasparotto, "Evaluation of two different methods to calibrate ultra-high value resistors at INRIM," *IEEE Trans. Instrum. Meas*., 60, 965- 970, 2011.

[13] B. Schumacher and J. Melcher, "Automated high-value resistance calibration up to 1 PΩ," Conference on Precision Electromagnetic Measurements, 635-636, June 13-18, 2010.

[14] G. Rietveld, D. G. Jarrett, and B. Jeckelmann, "Accurate High-Ohmic Resistance Measurement Techniques up to 1 PΩ," Conference on Precision Electromagnetic Measurements (CPEM), 290-291, 2014.

[15] E. O'Brien, D. G. Jarrett, and M. E. Kraft, "A 100 TΩ Guarded Hamon Transfer Standard," Conference on Precision Electromagnetic Measurements (CPEM), 294-295, 2014.

[16] A.E. Kennelly, "Equivalence of triangles and stars in conducting networks, Electrical World and Engineer," 34, 413–414, 1899.

[17] H. A. Sauer, "Wye-Delta Transfer Standards for Calibration of Wide Range dc Resistance and dc Conductance Bridges," *IEEE Trans. Instrum. Meas*., IM-17, 151-155, 1968.

[18] Y. Semenov and I. Samodurov, "Microwire-wound resistors in high value resistance measurements in VNIIM," Conference on Precision Electromagnetic Measurements (CPEM), 643-644, 2010.

[19] ISO GUM ISO/IEC Guide 98-3:2008 Uncertainty of measurement -- Part 3: Guide to the expression of uncertainty in measurement (GUM:1995)

[20] K. M. Yu, W. S. Kim, S. H. Lee, K. S. Han and J. H. Kang, "A method for measuring high resistances with negligible leakage effect using one voltage source and one voltmeter," *Meas. Sci. Technol*., 25, 075012, 2014.

[21] R. F. Dziuba, D. G. Jarrett, L. L. Scott, and A. J. Secula, "Fabrication of High-Value Standard Resistors," *IEEE Trans. Instrum. Meas*., 48, 333-337, 1999.

[22] K. M. Yu, D. G. Jarrett, S. U. Payagala, and M. E. Kraft, "A study of Wye-delta Networks for High Resistance," NCSLI, Grapevine, TX, USA, July 22, 2015

[23] D. G. Jarrett, S. U. Payagala, M. E. Kraft, K. M. Yu, 2016 Third Generation of Adapted Wheatstone Bridge for High Resistance *Proceedings of the 2016 Conference on Precision Electromagnetic Measurements (CPEM 2016)*, Ottawa, Canada

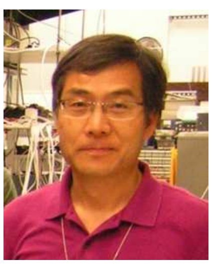

Kwang Min Yu was born in South Korea in 1960. He received the B.S. degree in physics, and the M.S. and Ph.D. degrees in solid-state physics from Pusan National University, Busan, South Korea. In 1986, he joined the Korea Research Institute of Standards and Science (KRISS), Daejeon, South Korea, where he has been involved in electrical resistance standards. He is currently a Senior Researcher with the Center for Electricity and Magnetism, KRISS.

Dean G. Jarrett was (S'88–M'90–SM'99) was born in Baltimore, MD, in 1967. He received the B.S. degree in electrical engineering from the University of Maryland, College Park, in 1990 and the M.S. degrees in electrical engineering and applied biomedical engineering from Johns Hopkins University, Baltimore, in 1995 and 2008, respectively.

Since 1986, he has been with the National Institute of Standards and Technology (NIST), in Gaithersburg, MD, where he was a Cooperative Education Student from the University of Maryland. During this time, he worked in the DC resistance area on the automation of resistance calibration systems. In 1991 he joined NIST full time as an electrical engineer working on the development of an automated AC resistance calibration system and the development of new resistance standards. Since 1994, Mr. Jarrett has worked in the high resistance laboratory developing automated measurement systems and improved standard resistors to support high resistance calibration services and key comparisons. In recent years, Mr. Jarrett has worked on sensor technologies for the detection of biological molecules and low-current source and measure techniques. Since 2014, he has led the Metrology of the Ohm Project at NIST.

Albert F. Rigosi (M'17) was born in New York, NY, USA in 1989. He received the B.A., M.A., M.Phil., and Ph.D. degrees in physics from Columbia University, New York, NY, in 2011, 2013, 2014, and 2016, respectively.

From 2008 to 2015, he was a Research Assistant with the Columbia Nano Initiative. From 2015 to 2016, he was a Joint Visiting Research Scholar with the Department of Applied Physics of Stanford University in Stanford, CA, and the PULSE Institute of SLAC National Accelerator Laboratory in Menlo Park, CA. Since 2016, he has been a Physicist at the National Institute of Standards and Technology in Gaithersburg, MD. His research interests include two-dimensional electron systems and applications of those systems' behaviors for electrical metrology.

Dr. Rigosi is a member of the American Physical Society and the Mellon-Mays Initiative of The Andrew W. Mellon Foundation. He was awarded associateships and fellowships from the National Research Council (USA), the Optical Society of America, the Ford Foundation, and the National Science Foundation (Graduate Research Fellowship Program).

Shamith U. Payagala received the B.S. degree in electrical engineering from the University of Maryland, College Park, MD, in 2015.

He joined the National Institute of Standards and Technology (NIST), Gaithersburg, MD, in 2014, and he serves as an Electrical Engineer for the Metrology of the Ohm project.

Marlin E. Kraft was born in Ransom, KS, in 1951. He received the A.S. degree in electronic technology from Kansas State University, Manhattan, KS, in 1980.

From 1980 to 2001, he was with Primary Standards Laboratory, Sandia National Laboratories. He specialized in all areas of dc metrology and was the Associate Project Leader.

From 2002 until retirement in 2018, he was with the National Institute of Standards and Technology (NIST) in Gaithersburg, MD, for the metrology of the ohm in the Fundamental Electrical Measurements group. His work with NIST involved dc current, high and low dc resistance, and dc high voltage.